ORIGINAL PAPER

Why don't branches snap? The mechanics of bending failure in three temperate angiosperm trees

A. van Casteren · W. I. Sellers · S. K. S. Thorpe ·
S. Coward · R. H. Crompton · A. R. Ennos

Abstract Living tree branches are almost impossible to snap. Some show "greenstick fracture", breaking halfway across before splitting along their length, while others simply buckle. In this study we investigated the bending failure of coppice branches of three temperate angiosperm trees: ash, *Fraxinus excelsior*; hazel, *Corylus avellana*; and white willow, *Salix alba*. We carried out bending tests, and made a series of observations on the structure, density and tensile and compressive strength of their wood to understand the pattern of failure. The three species showed contrasting behaviour; willow buckled whereas ash showed clean greenstick fracture and hazel a more diffuse greenstick fracture. These differences could be related to their wood properties. Willow buckled because its light wood had very low transverse compressive strength, particularly tangentially and was crushed by transverse stresses. Though the other species yielded in longitudinal compression on the concave side, they ultimately failed in tension on the convex side when bent because their higher density wood resisted transverse

compression better. However, the crack was diverted down the midline because of the low tangential tensile strength of their wood. Differences in fracture between ash and hazel are related to fine-scale differences in their wood anatomy and mechanics.

Introduction

It has long been noted that branches of different tree species fail in different ways when subjected to bending (Ennos and van Casteren 2010). Many fail by the typical "greenstick fracture" (Fig. 1a) in which tensile fracture occurs on the convex side but is unable to propagate throughout the branch to cause a complete break. In these branches, the crack extends to approximately the mid point of the branch where it then diverts into the longitudinal direction. Branches of some other species show quite different failure. They buckle, failing in transverse compression (Fig. 1b) and fracture does not occur at all. In a recent paper, Ennos and van Casteren (2010) suggested that these differences are due to the pattern of transverse stresses set up in beams when they are bent and the contrasting transverse mechanical properties of the wood. As well as the well-known longitudinal stresses that are set up when a beam is bent, transverse compressive stresses are also set up, though they can be ignored in most isotropic materials since these are much smaller than the longitudinal stresses (Ennos and van Casteren 2010). However, they can become important in wood, which is highly anisotropic. Buckling should occur in light wood, because the transverse compressive stresses can overcome its extremely low tangential compressive strength

Communicated by R. Matyssek.

A. van Casteren · W. I. Sellers · A. R. Ennos (✉)
Faculty of Life Sciences, University of Manchester,
Manchester M13 9PT, UK
e-mail: roland.ennos@manchester.ac.uk

S. K. S. Thorpe · S. Coward
School of Biosciences, The University of Birmingham,
Edgbaston, Birmingham B15 2TT, UK

R. H. Crompton
Musculoskeletal Science Research Group,
Institute of Aging and Chronic Disease, Sherrington Buildings,
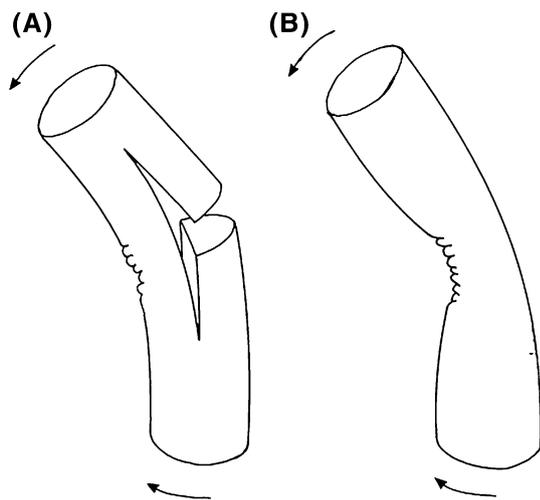The University of Liverpool, Liverpool L69 3GE, UK

Fig. 1 The two types of failure predicted for branches of different wood density (Ennos and van Casteren 2010). Dense wood should show greenstick fracture (**a**) as tensile fracture on the convex side is diverted along the central axis. In contrast light wood should result in buckling (**b**) as the transverse stresses set up cause the thin-walled cells to collapse

(Ennos and van Casteren 2010). In contrast, greenstick fracture should occur in denser wood which is less anisotropic; though the wood on the concave side should yield in longitudinal compression, it will not actually break, and tensile failure will then occur on the convex surface. The fracture should be diverted along the branch halfway through because of its low tangential tensile strength.

It is important to consider wood anatomy and structure in order to understand how a branch may fail in bending. The vast majority of tree cells are longitudinally arranged tubes that are well adapted for the conduction of water. However, because a tree is effectively a series of cantilevered beams, the trunk and branches have to resist bending forces. The longitudinal arrangement of the cells allows them to withstand the longitudinal stresses set up by such bending forces, which result mainly from the action of the wind. The cells act like pillars in compression and tensile ropes in tension and this gives wood its well-exploited strength along the grain (Ennos 2001; James et al. 2006; Reiterer et al. 2002). However, this arrangement makes wood a very anisotropic material; it is considerably stronger parallel to its longitudinal axis. This degree of anisotropy means that the transverse forces, usually ignored when considering bending and fracture of isotropic materials, are of some importance when considering the bending and fracture of wood.

To provide extra radial strength trees have rays; these are made up of living parenchyma cells. These structures have been shown to provide mechanical support to wood in the radial direction (Reiterer et al. 2002) preventing splitting between adjacent growth rings. In angiosperms the

arrangement of rays can vary between species. They can either be uniseriate, where the rays are only one cell thick, or they can be multiseriate, where the rays are two or more cells thick. Species also demonstrate a variety in the type, density and arrangement of ray cells in the wood structure which can affect the mechanical properties of the branch (Carlquist 1988; Reiterer et al. 2002). The greater the proportion of ray cells, the stronger the wood will be in the radial direction compared to the tangential direction. The growth pattern of wood is also important when considering the mechanics of branch failure. In angiosperms, which have differentiated vessels and fibres, the vessels are arranged in either a ring porous structure or a diffuse porous structure. In a ring porous tree the vessels are localised into well-defined rings that are laid down early in the growing season creating an "early wood"; here the abundance of large vessels means it is mechanically weaker than the remaining "late wood". In contrast, in diffuse porous trees the conducting vessels are distributed more evenly through the wood (Clarke 1933; Dresch and Dinwoodie 1996).

Density is one of the main factors controlling the mechanical properties of wood (Bowyer et al. 2003; Dresch and Dinwoodie 1996; Saranpaa 2003); the longitudinal strength and stiffness are in general directly proportional to density. A low-density wood will have a greater void volume and thinner cell walls than a high-density wood (Bowyer et al. 2003; Saranpaa 2003; Tsoumis 1991). As a result, density has an even greater effect on the transverse properties; light woods are much easier to split along their length and far easier to crush laterally because of the ease with which their thin walls can be buckled.

This paper aimed to investigate the differing modes of fracture of branches of three temperate angiosperm species (*Fraxinus excelsior*, *Corylus avellana* and *Salix alba*), and to explain the differences we found by relating them to the anatomy and mechanical properties of wood.

Materials and methods

Sample acquisition

Three species of commonly coppiced trees were chosen as the test subjects for this investigation: common ash (*F. excelsior*), common hazel (*C. avellana*) and the white willow (*S. alba*). Coppiced stands from *F. excelsior* and *C. avellana* stands were sourced from coppices at the University of Manchester's arboretum at Jodrell Bank and the *S. alba* stands were sourced from coppices at Sale Water Park. From being harvested the wood was kept hydrated at all times before and immediately up to testing.

Hand bending tests

Initial hand bending tests were conducted on samples of diameter 1.0–2.0 cm in diameter, from the three test species (*F. excelsior*, *C. avellana*, *S. alba*). Samples cut into 50 cm lengths were loaded in pure bending by manually applying a load by holding with right and left hands at each end and bending them until fracture occurred. The fracture was then classified into one of three pre-designated fracture types. These types were *diffuse fracture*, in which there were multiple fractures on the tensile side, with some small longitudinal cracking (Fig. 2a), *clean fracture*, in which there were limited clean fractures on the tensile side with large longitudinal cracks along the centre line (Fig. 2b); and *transverse buckling* in which there were no definitive fracture, but there was buckling in transverse compression (Fig. 2c). A χ^2 test was then run to see if there was a significant difference in the frequency of fracture types between the three species.

Bending experiments

A three point bending test was utilised to calculate the flexural modulus and the maximum longitudinal stress of intact branch lengths, all experiments being conducted on an Instron® universal testing machine (model 4301). The three-point bending apparatus had a maximum bending span of 26 cm and this was used for every bending sample. The effect of shear in three point bending can lead to an underestimation of the flexural stiffness. To limit this effect the samples therefore had to have a minimum span-to-depth ratio of 20 (Beismann et al. 2000; Vincent 1992). This meant that no sample could have a diameter of over 1.3 cm. Flexural bending tests were performed on sections of coppiced wood; ten stands were taken from each of the three test species. These stands were then cut into samples of 35 cm in length and with a maximum diameter of 1.3 cm for testing and laid on the supports of the three-point bending rig. The crosshead was then moved downwards at a speed of 35 mm min^{-1}, a central probe pushing down at the midpoint between the two supports, bending the branch while the restoring force was measured by a 1-kN load cell. An interfacing computer simultaneously recorded the force required and the displacement of the central probe. The flexural modulus and the maximum longitudinal stress of each section were then calculated by the Instron® machine using conventional engineering equations (Ennos 1991). The rigidity of the beam EI is given by the equation

$$\mathrm{EI} = \frac{dF}{dx}\frac{L^3}{48},\qquad(1)$$

where, dF/dx is the initial slope of the force displacement curve of the central probe and L is the distance between the
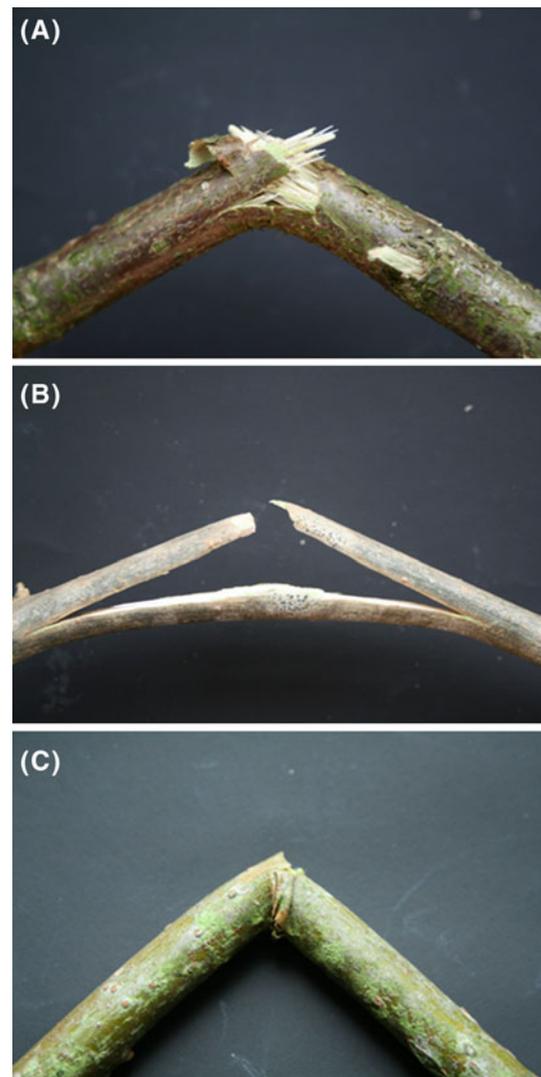

Fig. 2 The three typical modes of fracture. **a** *Diffuse fracture*, multiple tensile fractures with small to medium longitudinal cracks. **b** *Clean fracture*, limited clean fractures on the tensile side with large longitudinal cracks along the centre line. **c** *Transverse buckling*, no tensile fracture occurs and ample fails by buckling longitudinally and laterally

supports. The flexural modulus, E, of the wood was then calculated by dividing the rigidity by the second moment of area of the circular section, I, which is given by the equation

$$I = \pi r^4/4\qquad(2)$$

where, r is the radius.

The bending strength, M_{max}, of the beam is given by the equation

$$M_{max} = F_{max}L/4,\qquad(3)$$

where, F_{max} is the maximum force. Finally, the maximum longitudinal stress of the material in bending, σ_{Bmax}, is calculated using the equation

$$\sigma_{Bmax} = M_{max} r / I. \tag{4}$$

Tensile and compressive tests

The narrow stems were too small to yield wood specimens that could be subjected to mechanical testing, particularly transversely. For this reason, to measure the strength of the wood in different orientations, test specimens were cut from larger sections of wood (4–8 cm in diameter), though, of course being older this wood was likely to have rather different properties, being composed of less juvenile wood. Three different types of sample were cut for both compressive and tensile tests. One set was cut with a radial orientation, another set was cut with a tangential orientation and a third was cut with a longitudinal orientation.

Tensile samples were cut into a standard dumbbell shape for testing. The narrow central regions of the radial and tangential samples were on average 13.3-mm long, 4.5-mm wide and 5.2-mm thick. Due to the greater strength of wood along its longitudinal axis, the longitudinal samples were cut longer and thinner, being on average 30.0-mm long, 1.26-mm wide and 1.72-mm thick.

The compressive samples were simply cut into cuboids for testing, radial and tangential samples being on average 10.1-mm long, 8.5-mm wide and 8.2-mm thick. Longitudinally oriented samples were smaller so they did not to reach the limits of the 1-kN load cell; they were on average 4.2-mm long, 5.0-mm wide and 5.2-mm thick.

The cut samples were stored above distilled water in a sealed contain to ensure that hydration was maintained at 100% relative humidity until testing, which occurred within 2 days of cutting. All tensile and compressive tests were conducted on an Instron® universal testing machine. Tensile samples were clamped from above as well as below while compressive sample were placed on one stationary platform and compressed by a flat plate from above. The crosshead speed was set to 10 mm per second and the forces were measured using a 1-kN load cell. For tensile tests, wood strength is best quantified by determining its tensile breaking stress, σ_{Tmax}. This was calculated using the equation

$$\sigma_{Tmax} = F_{max} / WT \tag{5}$$

where, F_{max} was the breaking force and W and T were the width and thickness of the sample.

For compressive samples we used a more complex procedure to calculate the compressive strength of the wood. It is better to quantify this by calculating its compressive yield stress, rather than its breaking stress, because wood has biphasic behaviour in compression. As wood is crushed the force initially rises linearly with the applied load as in tension; however, rather than break, the wood yields (Fig. 3) as the cell walls collapse, and the slope of the force/displacement graph falls dramatically. Finally, as
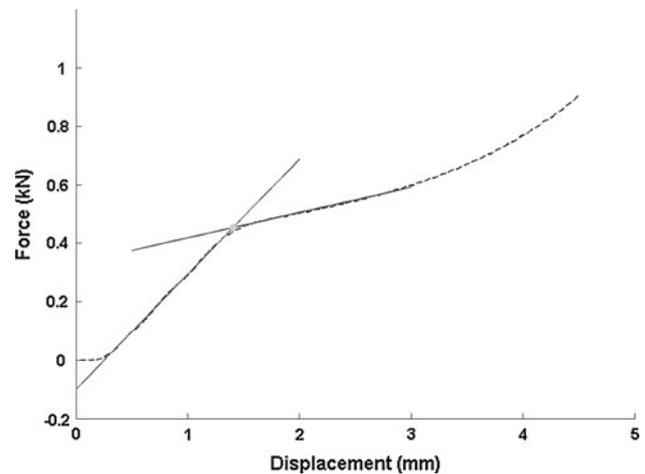

Fig. 3 An example of the method used to calculate the yield force during compressive testing. The slope for the initial linear region and region after the yield point was calculated and two lines were drawn. The point at which these lines crossed was deemed to be the yield force; this was then divided by the cross-sectional area of the sample to give the yield stress (MPa)

crushing continues the cell walls get packed together and the force required increases as the material is densified. To calculate yield stress the data was entered into Matlab and a graph of force versus displacement was generated. The slope of the initial linear region was then calculated and a line drawn; the slope of the line after the yield point was then also calculated and a line drawn. The point at which these lines crossed was deemed to be the yield force F_{yield}, (Fig. 3). The compressive yield stress, σ_{Cyield}, was then calculated using the equation

$$\sigma_{Cyield} = F_{yield} / WT \tag{6}$$

where, W and T were the width and thickness of the sample.

The stiffness of samples was not recorded because the compliance of the Instron® machine itself would mean the recordings would be subject to large errors.

Density measurements

The density was directly measured for all of the radial and tangential specimens. Density was calculated by dividing the dry weight of samples by the fresh volume. To obtain the fresh volume, Archimedes' principle was employed. The weight of a container of distilled water standing on a balance was measured before and after fully submersing a wood specimen. The wood volume was calculated by dividing the difference in the two weights by the density of water (0.998 g cm^{-3}) (Hacke et al., 2000). To obtain the dry weight, the samples were then placed into an oven at 65°C and allowed to dry for a minimum of 72 h. Once dry, the weights were measured using an electronic balance.

Table 1 Table showing the frequency of different sorts of failure in the three species and the results of the χ^2 analysis, showing that different woods are more prone to different sorts of failure

Species	Diffuse fracture O (E)	Clean fracture O (E)	Transverse buckling O (E)	Total
Fraxinus excelsior	9 (7.53)	16 (8.21)	1 (10.26)	26
Corylus avellana	11 (5.50)	8 (6.00)	0 (7.50)	19
Salix alba	2 (8.97)	0 (9.79)	29 (12.24)	31
Total	22	24	30	**76**
χ^2	67.858			
df	4			
Crit value	9.48			

Scanning electron microscopy

Using a scanning electron microscope (SEM, Cambridge 360) and Environmental scanning electron microscope (ESEM, Philips XL30 ESEM-FG), images were taken of the fracture surfaces from hand bending samples of both the *F. excelsior* and *C. avellana* specimens. Due to the method of failure in willow there was no visible fracture surface. In this case a cross section along the longitudinal axis was created by cutting the sample; this revealed the compressive failure that occurred in the sample. The specimens were air dried, attached to an aluminium stub with double sided sticky carbon tabs and then coated with gold. Using the SEM and ESEM, high-magnification images were then taken to image how the fracture had occurred.

Data analysis

Calculation of the mechanical properties was performed, in the main part, by the Instron® universal testing machine, except for the yield stress in compression (see *Tensile and Compressive Testing* for methods). All statistical tests were performed on SPSS statistical program apart from the χ^2 test, which was performed by hand.

Results

Hand bending tests

The numbers of sections of each species that failed by each mode of fracture are shown in Table 1, which also gives the results of the χ^2 test. As the χ^2 value is far greater than the critical value of χ^2 at 5%, we must reject the null hypothesis and say that the distribution of the fracture mechanisms is significantly different from the expected values if there was a homogenous distribution of fracture mechanisms between species. In particular many more *F. excelsior* samples failed by clean fracture than expected, many more *C. avellana* samples failed by diffuse fracture, and many more *S. alba* samples failed by transverse buckling.

Mechanical testing

Wood density

The mean wood densities were significantly different between species ($F_{119} = 24.720$, $P < 0.00$). At 492 (S.E. 20) kg m^{-3} and 505 (S.E. 20) kg m^{-3}, a Tukey's test showed that the wood of both *F. excelsior* and *C. avellana* were significantly denser than that of *S. alba* (436 (S.E. 20) kg m^{-3}) but not significantly different from each other.

Three-point bending tests

The results from the three-point bending tests are displayed in Fig. 4a, b. There were significant differences between species in flexural modulus ($F_{135} = 33.680$, $P < 0.000$), a Tukey's test showing that *S. alba* had a significantly higher flexural modulus than the other two species tested, although all species were significantly different from each other. The results for the maximum longitudinal stress showed a different pattern (Fig. 4b); though again there were differences between species ($F_{136} = 8.999$, $P < 0.000$), in this case *S. alba* had the lowest maximum stress of all the species tested; however, the Tukey's test showed that it was only significantly lower than *C. avellana*.

Wood tests

The results of the transverse tensile tests performed on all three species are displayed in Fig. 5. A two-way ANOVA showed that in all species the wood was significantly stronger in the radial direction than in the tangential direction ($F_1 = 83.212$, $P < 0.000$). *Salix alba* had significantly lower tensile breaking stress than the other species tested ($F_2 = 16.199$, $P < 0.000$).

The results of transverse compression tests demonstrating the compressive yield stress (MPa) are presented in Fig. 6. Once again there were significant differences between the samples tested in a radial direction and samples tested in a tangential direction, radial samples being stronger than tangential ones ($F_1 = 13.622$, $P < 0.001$). *Salix alba* also demonstrated a significantly ($F_2 = 102.070$, $P < 0.000$) lower mean compressive yield stress than all the other species in any orientation; its compressive
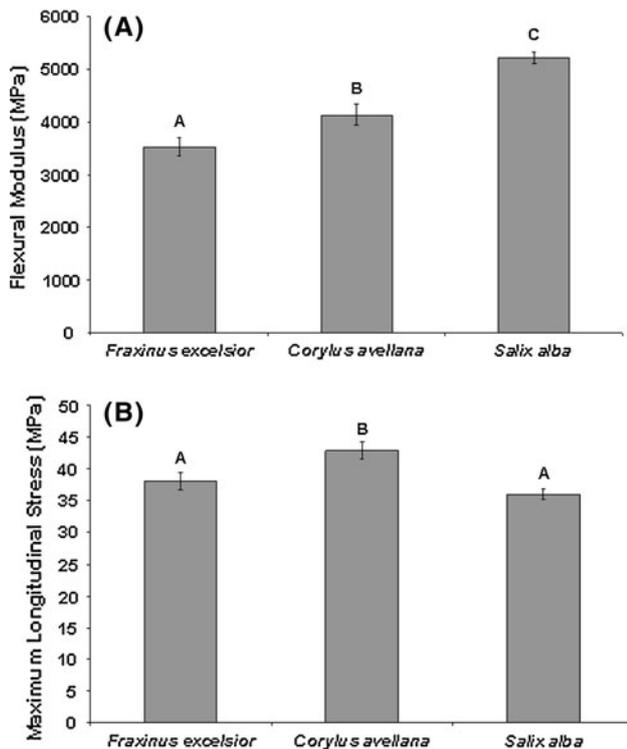
Fig. 4 **a** The mean flexural modulus calculated from the three-point bending test. *Fraxinus excelsior* $n = 35$, *Corylus avellana* $n = 34$, *Salix alba* $n = 65$. *Error bars* represent standard error. There were significant differences between species in flexural modulus ($F_{135} = 33.680$, $P < 0.000$). Results of post hoc Tukey tests are denoted using *letters*; columns labelled with the same letter display no significant difference. **b** The mean maximum longitudinal stress calculated from the three-point bending tests. *Fraxinus excelsior* $n = 35$, *Corylus avellana* $n = 36$, *Salix alba* $n = 65$. *Error bars* represent standard error. There were differences between species ($F_{136} = 8.999$, $P < 0.000$). Results of post hoc Tukey tests are denoted using *letters*; columns labelled with the same letter display no significant difference

strength was only around 40% of the other species in this study.

The results of longitudinal tensile and compression tests are shown in Fig. 7. It can be seen that the tensile breaking strength of wood is around three to five times higher than the compressive yield stress. Again *S. alba* has a significantly lower strength than the other species tested in both tensile ($F_{29} = 41.179$, $P < 0.00$) and compression ($F_{29} = 20.506$, $P < 0.001$) tests. The tensile and compressive strengths in the longitudinal direction are many times higher than the corresponding strengths in the transverse directions.

Discussion

The results of the statistical analysis of the preliminary hand bending tests agreed with anecdotal observations that
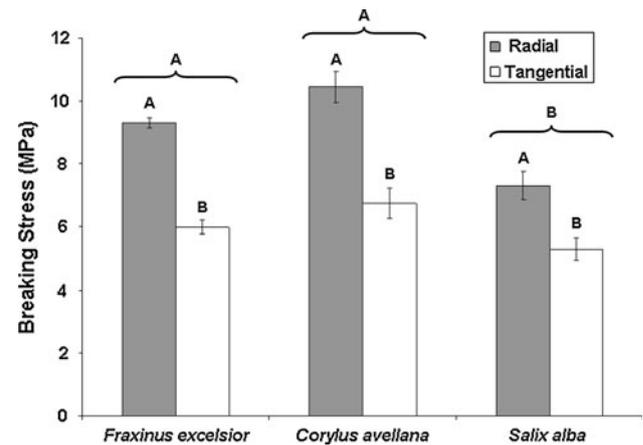

Fig. 5 The mean transverse tensile breaking stress of wood sample tested in both a radial orientation and a tangential orientation. All groups $n = 10$. *Error bars* represent standard error. A two-way ANOVA showed that in all species the wood was significantly stronger in the radial direction than in the tangential direction ($F_1 = 83.212$, $P < 0.000$). *Salix alba* demonstrated significantly lower tensile strength than the other species tested ($F_2 = 16.199$, $P < 0.000$). Results of post hoc Tukey tests are denoted using *letters*; columns labelled with the same letter display no significant difference

branches of the three species of trees tested in this study (*F. excelsior*, *C. avellana*, *S. alba*) did fail in different ways when bent (Table 1). This then poses two main questions: how do these modes of failure differ from each other; and what are the causes of these differing fractures?

In *C. avellana,* though the failure began with longitudinal compressive yield on the concave side, it then failed in tension on the convex side and this generated multiple fractures and many small longitudinal cracks (Fig. 8a). This tensile failure did not run through the beam but stopped around the mid-point in the majority of cases. Under higher magnification the fracture was shown to be quite random and the location of fractures did not seem to be dictated by the wood anatomy (Figs. 2a, 8b). The fracture of *F. excelsior* was rather different; the fracture ran straight, directly across the convex side of the branch, though, as in *Corylus* it did not extend completely across the beam. Failure in *F. excelsior* also generated a much more substantial longitudinal crack along the mid-point and the fracture appeared to be cleaner when compared with the fracture of *C. avellana* (Fig. 2b). In *F. excelsior* there were also other lengthy longitudinal cracks and these occurred at the junctions between late wood and the next year's early wood (Fig. 9a, b).

In neither *C. avellana* nor *F. excelsior* did the branch snap completely across; instead the failure stopped around the mid-point of the branch. This type of fracture has been noted previously in branches (Ennos and van Casteren 2010) and is probably due to the anisotropy of the material. Both tensile and compressive tests (Figs. 5–7) show that in
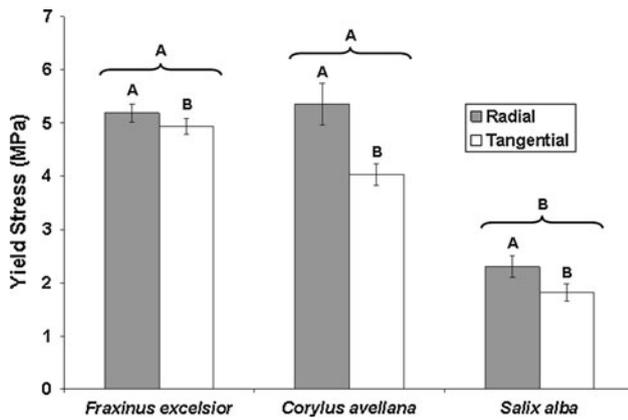
Fig. 6 The mean transverse compressive yield stress of wood samples in both the radial and tangential orientation. All groups $n = 10$. *Error bars* represent standard error. Two way ANOVA showed that in all species there were significant differences between the samples tested in a radial direction and samples tested in a tangential direction ($F_1 = 13.622$, $P < 0.001$). *Salix alba* demonstrated a significantly ($F_2 = 102.070$, $P < 0.000$) lower mean yield stress than all the other species. Results of post hoc Tukey tests are denoted using *letters*; columns labelled with the same letter display no significant difference
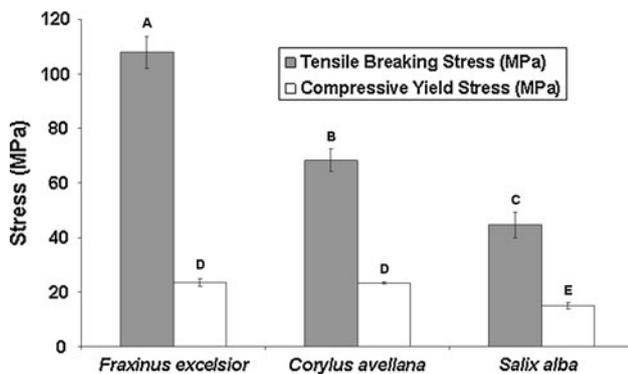

Fig. 7 The mean longitudinal tensile breaking stress and compressive yield stress of wood samples. In all groups $n = 10$ and *error bars* represent standard error. ANOVA tests showed that *Salix alba* has a significantly lower strength than the other species tested in both tensile ($F_{29} = 41.179$, $P < 0.00$) and compression ($F_{29} = 20.506$, $P < 0.001$) tests. Results of post hoc Tukey tests are denoted using *letters*; columns labelled with the same letter display no significant difference

all three species the wood is much stronger longitudinally than transversely, probably because most xylem cells are oriented longitudinally. Strength is the lowest of all in the tangential direction, probably because the rays provide a little or no mechanical support in this orientation. These results agree with the previous work on wood mechanics (Dresch and Dinwoodie 1996; Bowyer et al. 2003) and the experiments of Reiterer et al. (2002) on the effect that ray tissue has on the mechanical and fracture properties of wood. Reiterer et al. (2002) showed that, in tensile tests,
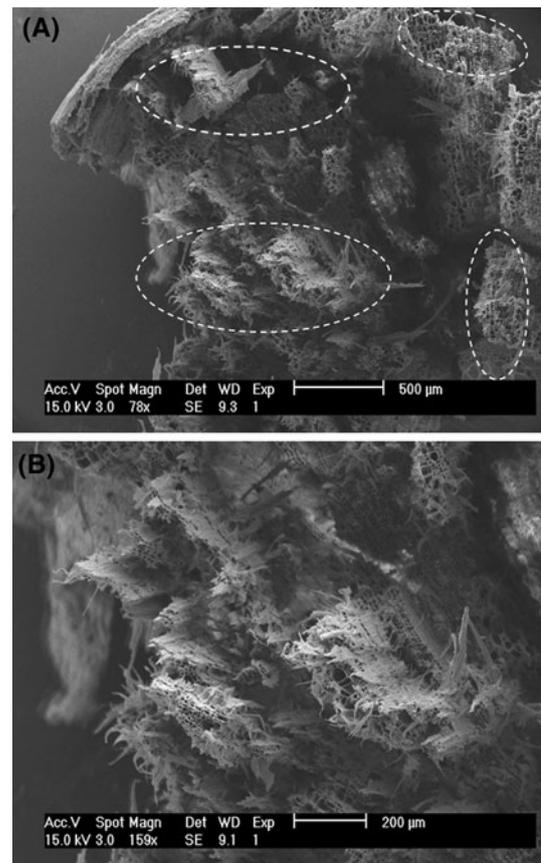

Fig. 8 ESEM images of the tensile fractures of *Corylus avellana*, taken from a longitudinal orientation. **a** A tensile fracture in *Corylus avellana*, *circled areas* show that where fracture occurs it does not occur along vessels, but appears to be dispersed throughout the sample. **b** Higher magnification of *one circled area* demonstrating the large amount of fibre pullout and the lack of an ordered pattern of failure

radial strength was around 60% higher than tangential strength in both *F. excelsior* and *Quercus robur*.

Our results showed that the longitudinal strength of *F. excelsior* wood in tension is around 12 and 18 times higher than radially and tangentially, respectively, whilst figures for *C. avellana* are 6.5 and 10 times higher. The Cook–Gordon model of crack propagation states that as a crack moves through a material the tensile stress parallel to its length are one-fifth of those at right angles to the tip. Consequently when a branch is breaking across its length, the low transverse tensile strengths of the wood would cause the crack to be diverted in a longitudinal direction, as demonstrated in the hand bending fractures of both *F. excelsior* and *C. avellana*. The crack would be able to travel most easily exactly through the centre of the branch, where it does not have to cross any ray cells, and at junctions of growth rings, where material is weaker (Ennos and van Casteren 2010). The reason for the larger longitudinal cracks in *F. excelsior* is probably because it has a
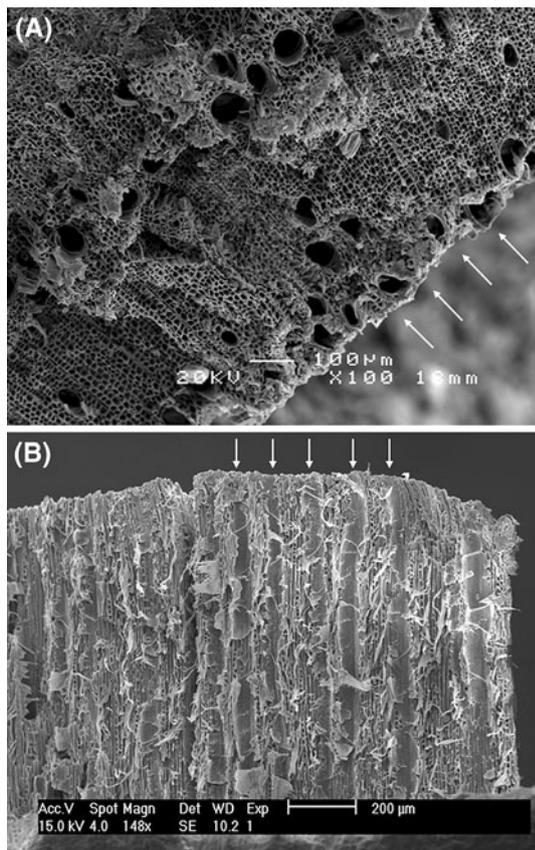
Fig. 9 **a** An SEM image demonstrating the fracture of *Fraxinus excelsior* showing how the fracture has occurred along the boundary between early and late wood, highlighted using *arrows*. Image is of a transverse cross section. **b** An ESEM image of the topside of a fracture in *Fraxinus excelsior* showing that the fracture has occurred along the larger early wood vessels, *arrows* indicate where these vessels are positioned. Image is of a tangential cross section

Fig. 10 ESEM images of a radial section of *Salix alba* parallel to the axis of bending. (**a**) Showing the compression crease (indicated with an *arrow*) of the transverse buckling mode of failure. **b** A higher magnification of the crushed cells in the crease

greater ratio between longitudinal and tangential tensile strength: 18:1 in *F. excelsior* compared with only 10:1 in *C. avellana* (Fig. 7).

The differences in transverse wood strength of the two species are in turn probably due to their differences in anatomy. *Corylus avellana* is often described as having diffuse porous wood (Metcalfe and Chalk 1983), in contrast to *F. excelsior* that demonstrates a clear ring porous pattern, of light early wood and denser late wood (Clarke 1933). The large vesseled early wood is known to be weaker and more compliant than the denser late wood (Dresch and Dinwoodie 1996; Mattheck and Kubler 1995; Zink-Sharp 2003); the junction between early and late wood is therefore a mechanical weak point (Clarke 1933; Mattheck and Kubler 1995). The difference in stiffness should also result in stress concentrations being built up there. This could be the reason why longitudinal cracks are localised along the growth rings of *F. excelsior* (Fig. 9a, b). In contrast, in the more diffuse porous wood of *C. avellana*
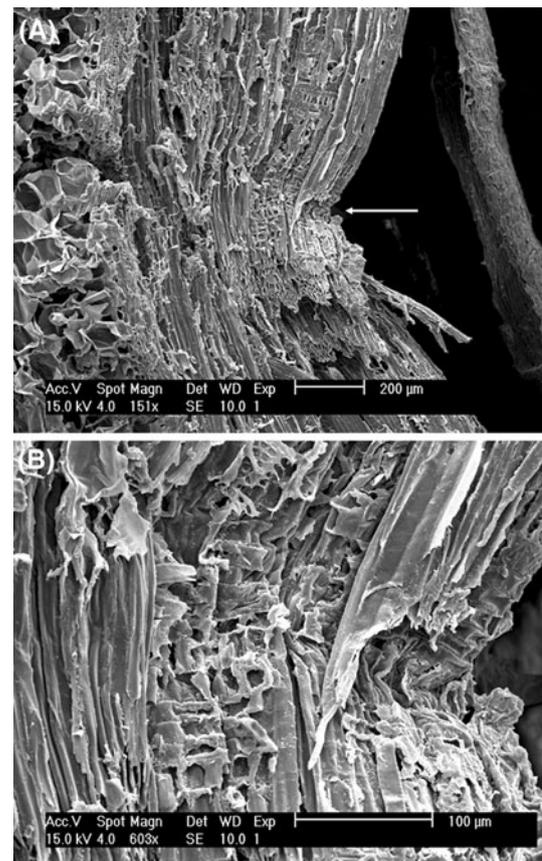
no ordered patterns of fracture are produced because there are no lines of weakness except along the midline of the branch; the facture surface could be diverted by small-scale irregularities, such as around individual vessels or around individual fibres. Small-scale differences in ray density may also have contributed to the different types of fracture. Although both *F. excelsior* and *C. avellana* both have multiseriate rays the density of rays varies between species. *Fraxinus excelsior* has been shown to have between 5 and 9 ray cells per tangential mm whilst *C. avellana* is shown to have between 15 and 19 ray cells per tangential mm (Metcalfe and Chalk 1983; Richter and Dallwitz 2000). Adding to this the genus Corylaceae which includes *C. avellana* are reported to have very wide rays (Carlquist 1988). Alternatively, the difference in fracture may be related to differences in attachment between the individual fibres; the fibres may be better glued together in ash, a famously resilient wood, whereas in hazel the fibre pullout suggests poorer attachment.

Salix alba showed very different mechanical behaviour that was probably related to its lower wood density. Despite having lighter wood it actually had higher

longitudinal stiffness than the other species; this may be due to a lower microfibril angle in its cell walls which could increase longitudinal reinforcement (Huang et al. 2003; Saranpaa 2003). *Salix alba* also showed a very different pattern of failure; it did not fracture like the other two species tested, but failed by buckling transversely, (Figs. 2c, 10). The reason for this different pattern of failure in *S. alba is* probably related to its lower wood density. At lower densities, wood strength falls (Huang et al. 2003), particularly transversely. *S. alba* consequently demonstrated lower wood strength in all directions, both longitudinally and transversely, and in particular its wood had a much lower transverse compressive strength, with yield stresses only around 40% of the other two species. The theory developed by Ennos and van Casteren (2010) predicts that this low tangential compressive strength would allow the wood to buckle inwards in response to the transverse compressive transverse stresses that are set up during bending. Such buckling would occur well before the branch failed in tension on its convex side. This is presumably the reason why willow twigs can so readily be woven into baskets.

This study has demonstrated therefore that the differences between the modes of failure in three tree species (*F. excelsior*, *C. avellana*, *S. alba*) can be explained by their different density, mechanical properties and wood anatomy. Further studies may show how and why tropical woods with a much wider range of densities fail in bending.

References

Beismann H, Wilhelmi H, Bailleres H, Spatz H-C, Bogenrieder A, Speck T (2000) Brittleness of twig bases in the genus Salix: fracture mechanics and ecological relevance. J Exp Bot 51:617–633

Bowyer JL, Shmulsky R, Haygreen JG (2003) Forest products and wood science: an introduction. Iowa State Press, Iowa

Carlquist S (1988) Comparative wood anatomy. Springer-Verlag, Berlin

Clarke SH (1933) On estimating the mechanical strength of the wood of ash (*Fraxinus excelsior L.*). For 7:26–31

Dresch HE, Dinwoodie JM (1996) Timber; structure, properties, conversion and use. Macmillan Press, London

Ennos AR (1991) The mechanics of anchorage in wheat *Triticum aestivum L.*: II. Anchorage of mature wheat against lodging. J Exp Bot 2:1607–1613

Ennos AR (2001) Trees. The Natural History Museum, London

Ennos AR, van Casteren A (2010) Transverse stresses and modes of failure in tree branches and other beams. Proc Roy Soc Lond B 277:1253–1258

Hacke UG, Sperry JS, Pittermann J (2000) Drought experience and cavitation resistance in six shrubs from the Great Basin, Utah. Basic Appl Ecol 1:31–41

Huang CL, Lindström H, Nakada R, Ralston J (2003) Cell wall structure and wood properties determined by acoustics—a selective review. Holz als Roh- und Werkstoff 61:321–335

James KR, Haritos N, Ades PK (2006) Mechanical stability of trees under dynamic loads. Am J Bot 93:1522–1530

Mattheck C, Kubler H (1995) Wood: the internal optimization of trees. Springer, Berlin

Metcalfe CR, Chalk L (1983) Anatomy of the Dicotyledons, 2nd edn. Claredon Press, Oxford

Reiterer A, Burgert I, Sinn G, Tschegg S (2002) The radial reinforcement of the wood structure and its implication on mechanical and fracture mechanical properties—a comparison between two tree species. J Mater Sci 37:935–940

Richter HG, Dallwitz MJ (2000) Commercial timbers: descriptions, illustrations, identification, and information retrieval. In English, French, German, and Spanish, vol. 2009 http://www.biologie.uni-hamburg.de/b-online/wood/english/index.htm

Saranpaa P (2003) Wood density and growth. In: Jeronimidis G, Barnett JR (eds) Wood quality and its biological basis. Blackwell Publishing, Oxford

Tsoumis G (1991) Science and technology of wood. van Nostrand Reinhold, New York

Vincent JFV (1992) Biomechanics materials a practical approach. Oxford University Press, Oxford

Zink-Sharp A (2003) The mechanical properties of wood. In: Jeronimidis G, Barnett JR (eds) Wood quality and its biological basis. Blackwell Publishing, Oxford